MAGNETIC RESONANCE IN CHEMISTRY
Magn. Reson. Chem. **37**, 203–213 (1999)

Measurement of the deuterium relaxation times in double-labeled ($^{13}C/^{2}H$) thymidine and 2′-deoxyadenosine and in the selectively labeled DNA duplex $^{5'}d(^{1}C^{2}G^{3}\underline{A}^{4}\underline{T}^{5}\underline{T}^{6}\underline{A}^{7}\underline{A}^{8}\underline{T}^{9}C^{10}G)_{2}^{3'}$

T. V. Maltseva, A. Földesi and J. Chattopadhyaya*

Department of Bioorganic Chemistry, Box 581, Biomedical Center, Uppsala University, S-571 23 Uppsala, Sweden

ABSTRACT: The T_1 and $T_{1\rho}$ of deuterium in $^{13}C/^{2}H$ double-labeled 2′(*R*/*S*),5′(*R*/*S*)-$^{2}H_2$-1′,2′,3′,4′,5′- $^{13}C_5$-2′-deoxyadenosine and the corresponding thymidine derivative as well as in the non-uniformly labeled (shown in bold and underlined) DNA duplex, $d^{5'}(^{1}C^{2}G^{3}\underline{A}^{4}\underline{T}^{5}\underline{T}^{6}\underline{A}^{7}\underline{A}^{8}\underline{T}^{9}C^{10}G)_{2}^{3'}$, have been determined for the first time. These double-labelled nucleoside blocks have a special feature in that the geminal 2′–2″ and 5′–5″ proton–proton couplings are eliminated by replacement with diastereomeric deuterium at C-2′ and C-5′ centers. This uniquely enables us to perform deuterium relaxation measurement experiments through selective polarization transfer, $^{1}H–^{13}C–^{2}H–^{13}C–^{1}H$ at C-2′ and C-5′ centers, thereby allowing filtration of all other naturally abundant methylene- and methine-^{13}C as well as enriched methine-^{13}C fragments. Comparison of T_1 and $T_{1\rho}$ of ^{2}H in double-labeled ($^{13}C/^{2}H$) 2′-deoxyadenosine and thymidine with that of the non-uniformly labeled DNA duplex, $d^{5'}(^{1}C^{2}G^{3}\underline{A}^{4}\underline{T}^{5}\underline{T}^{6}\underline{A}^{7}\underline{A}^{8}\underline{T}^{9}C^{10}G)_{2}^{3'}$, shows that the dynamics of various nucleotide residues are indeed non-uniform.

KEYWORDS: relaxation times; deuterium; labeled DNA; dynamics

Received 26 June 1998; revised 5 October 1998; accepted 5 October 1998

INTRODUCTION

Nuclear magnetic resonance spectroscopy is one of the most powerful methods for studying intramolecular dynamics[1] both in solution and in the solid phase. NMR relaxation measurements are sensitive to a wide range of motional time-scales (from picoseconds to seconds) and provide information regarding reorientational motions of molecular axes and internuclear vectors. Relaxation measurements of ^{15}N,[2] ^{13}C[2] and/or ^{2}H[3–5] have been extensively performed for characterizing the dynamics of proteins.[2–5] For oligo-DNA or RNA, such relaxation measurement has traditionally been difficult to perform because of limited accessibility of appropriate non-uniform isotope-labeled substances.[6] Uniformly ^{13}C-labeled RNA[7] and DNA,[8a–c] however, have recently been found to be very useful for this purpose. The advantages of uniform ^{13}C labeling for structural studies on DNA and RNA include (1) relaxation measurements, (2) homo- and heteronuclear *J*-coupling analysis using polarization transfer through ^{13}C[8c] compared with traditionally used DQF COSY-type experiments and (3) for the reduction of the overcrowding of proton resonances by editing through the third ^{13}C dimension.[8a] The relaxation rate measurement of ^{13}C nuclei in uniformly labeled DNA/RNA is problematic because of the extra relaxation pathways such as DD($^{13}C–^{13}C$)[7b] or cross-relaxation of $^{13}C–^{1}H$ in the methylene fragment, which can be circumvented by selective ^{13}C enrichment at C-1′ and/or C-5′ in an oligo-DNA.[8d–f]

Clearly, the chemosphecific incorporation of deuterium at C-2′ and C-5′ in the uniformly ^{13}C-labeled sugar moieties in oligo-DNA and RNA will provide opportunities to perform relaxation studies on both deuterium and ^{13}C, thereby increasing the number of actual experimental datasets for the determination of the complex three-parameter spectral density function. This will also, in turn, reduce the number of assumptions which are usually made in order to compute all possible relaxation processes. The chemospecific incorporation of deuterium at C-2′ and C-5′ in the ^{13}C-labeled sugar moiety has three benefits. (1) They help to eliminate the geminal H-2′–H-2″ and H-5′–H-5″ couplings, facilitating the homo- and heteronuclear *J*-coupling analysis. (2) This also effectively helps to eliminate the cross-correlation effect of DD($^{13}C-^{1}H$) from the ^{13}C relaxation rate of methylene protons. (3) As stated above, the deuterium relaxation rates of the same methylene fragment provide an additional experimental dataset in addition to those derived from ^{13}C relaxation measurements, facilitating the computation of all relax-

* Correspondence to: J. Chattopadhyaya, Department of Bioorganic Chemistry, Box 581, Biomedical Center, Uppsala University, S-751 23 Uppsala, Sweden.
Contract/grant sponsor: Swedish Board for Technical Engineering Research (TFR).
Contract/grant sponsor: Swedish Natural Science Research Council; *Contract/grant number:* K-KU 12067-300; *Contract/grant number:* K-AA/Ku04626-321.
Contract/grant sponsor: Wallenbergsstiftelsen.
E-mail: jyoti@bioorgchem.uu.se.

 CCC 0749–1581/99/030203–11 $17.50

ation processes. Clearly, the description of the spectral density function will have increasing level of complexity[8d–f] as we learn to take into account of both slower and fast internal motions more precisely. It is therefore important to use as much experimental information (such as the relaxation rates of ^{2}H and ^{13}C together) as possible to reflect the overall and local relaxation processes more precisely and closer to reality.

The deuterium relaxation, in comparison with the ^{13}C relaxation, is governed by the following. (i) The only effective mechanism for deuterium is the quadrupolar relaxation[1] [$T_1{}^D \approx T_1{}^O$ and $T_2{}^D \approx T_2{}^O$], whereas ^{13}C has multiple mechanisms involved in its relaxation.[1] (ii) The role of cross-relaxation and cross-correlation mechanisms in the overall relaxation of deuterium has been found[3a] to be negligible compared with ^{13}C. (iii) In the approximation of the isotropic motion, the global correlation time, τ_c, can be calculated directly for deuterium from Eqns (1) and (2) using experimentally determined $T_1{}^D$ and/or $T_2{}^D$, if the quadrupolar coupling constant and the asymmetry parameter η are known.

The quadrupolar NMR relaxation rates for deuterium in the absence of chemical exchange can be defined as follows:[1,3]

$$\frac{1}{T_1{}^Q} = A[2J(\omega_{2H}) + 8J(2\omega_{2H})] \quad (1)$$

and

$$\frac{1}{T_2{}^Q} = A[3J(0) + 5J(\omega_{2H}) + 2J(2\omega_{2H})] \quad (2)$$

where

$$A = \frac{3\pi^2}{20}\left(\frac{qQe^2}{h}\right)^2\left(1 + \frac{\eta^2}{3}\right)$$

[(qQe^2/h) is the quadrupolar coupling, which is unknown, but solid-state NMR data for nucleosides show that it may vary between 160 and 200 kHz[9,10d] for ^{2}H(2′), ω_{2H} is the angular Larmor frequency of deuterium, η is the asymmetry parameter, which is very small, and $(1 + \eta^2/3)$ is close to unity].

Nevertheless, the DNA molecule should be described as a cylinder rather than an isotropic molecule with an asymmetric top and an axially symmetric diffusion tensor with two diffusion coefficients: $D_\perp = D_{xx} = D_{yy}$ and $D_\parallel = D_{zz}$.[2a,10] The spectral density function includes the dependence on the angle, ϕ between the ^{13}C–^{2}H bond and the principal frame of the diffusion tensor:

$$J(\omega) = \sum_{j=1}^{3} A_j \frac{\tau_j}{1 + \omega^2\tau_j{}^2}$$

where $\tau_1^{-1} = 6D_\perp$, $\tau_2^{-1} = 5D_\perp + D_\parallel$, $\tau_3^{-1} = 2D_\perp + 4D_\parallel$, $A_1 = 0.25\,(3\cos^2\phi\text{-}1)^2$, $A_2 = 3\sin^2\phi\cos^2\phi$ and $A_3 = 0.75\sin^4\phi$.

Hence the knowledge of deuterium relaxation, in conjunction with ^{13}C relaxation, would enable us to define the angle between the ^{13}C–^{2}H vector or the ^{13}C–^{1}H vector and the unique axis of the diffusion tensor. Since 2′- and 5′-methylene fragments are essential constitutents in the structural integrity and architecture of DNA molecule, the determination of diffusion anisotropy of both methylene fragments for each nucleotide residue (the 5′-methylene gives information about phosphate backbone whereas the 2′-methylene is expected to give information on the endocyclic sugar torsions) will allow the determination of long-range order in the NMR structure of DNA and its complexes with various ligands.[10b]

Whereas several reports of dynamic studies of oligo-DNA in the solid state[9] based on deuterium relaxation have appeared, dynamic studies by ^{2}H relaxation in solution have been performed only for proteins,[3–5] not for oligo-DNA. We report here the first ^{2}H relaxation study [T_1 and $T_{1\rho}$ of 2′(*R*/*S*),5′(*R*/*S*)-$^2H_2$-1′,2′,3′,4′,5′-$^{13}C_5$-2′-deoxyadenosine (**1**) and the corresponding thymidine (**2**) (bearing diastereomeric proton and deuteron in a 1:1 ratio at C-5′ and 15% (*R*): 85% (*S*) at C-2′] and also in the non-uniformly labeled DNA duplex, $d^{5'}(^1C^2G^3\underline{\mathbf{A}}^4\underline{\mathbf{T}}^5\underline{\mathbf{T}}^6\underline{\mathbf{A}}^7\underline{\mathbf{A}}^8\underline{\mathbf{T}}^9C^{10}G)_2^{3'}$ (**3**) (Fig. 1), in aqueous solution. The sites of incorporation of ^{13}C/^{2}H double-labeled dA and T blocks in the duplex (**3**) are shown in bold and underlined, and were achieved by the solid-phase synthesis protocol. The main reason for the choice of the oligo-DNA (**3**) in our study is because it has been shown (by x-ray and NMR analysis) that small modifications in the base pairing sequence (e.g. the substitution of the GC base pair in CGATTAATCG with CG in CCATTAATGG) causes a dramatic change in their minor groove structure and hydration

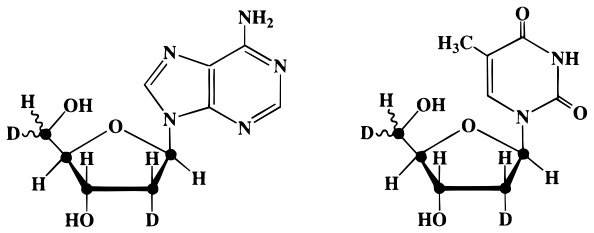

(1): dA **(2): T**

$$^{5'}d(^1C^2G^3\underline{\mathbf{A}}^4\underline{\mathbf{T}}^5\underline{\mathbf{T}}^6\underline{\mathbf{A}}^7\underline{\mathbf{A}}^8\underline{\mathbf{T}}^9C^{10}G)_2{}^{3'}$$

(3)

Figure 1. Diastereoselectively deuterated 2′(*R*/*S*),5′(*R*/*S*)-$^2H_2$-1′,2′,3′,4′,5′-$^{13}C_5$-2′-deoxyadenosine (**1**) and the corresponding thymidine (**2**) derivative (99 at% ^{13}C enriched sugar carbons are shown by solid black circles). C-5′ in both **1** and **2** has a 1:1 ratio of deuterioisotopomer, whereas the deuterium isotopomer ratio, 2′-^{2}H to 2″-^{2}H, is 15:85 at C-2′. The oligo-DNA duplex (**3**) is non-uniformly labeled with blocks of type **1** and **2** and they are shown by bold and underlined.

pattern,[11] although they both have the same AT tract. Naturally, an important question here is to address what the dynamic difference between these two duplexes is. The results presented in this paper constitute the first report of research in that direction.

Results and discussion

NMR experiment

The T_1 and $T_{1\rho}$ of ^{2}H in 2′(*R*/*S*),5′(*R*/*S*)-$^2H_2$-1′,2′,3′,4′,5′-$^{13}C_5$-2′- deoxyadenosine (dA) (**1**) and in the corresponding thymidine (T) derivative (**2**) were measured using the pulse sequences presented schematically in Fig. 2. The approach is basically very similar to the previously described methodology[3b] for measuring deuterium relaxation times in CHD methylene and CH_2D methyls of proteins.[3b] However, compared with earlier published sequences,[3b] we implemented a small modification because of the presence of ^{13}CHD methylene groups only at the 2′-and 5′-positions in our oligo-DNA: after the polarization transfer step between points (a) and (b)

$$\left(^1\mathrm{H} \xrightarrow{J_{CH},\ 90^\circ} \xrightarrow{90^\circ(^1\mathrm{H})} \xrightarrow{90^\circ(^{13}\mathrm{C})}\right)$$

in Fig. 2, the element $\tau_b - {}^1\mathrm{H}90_x^\circ 90_\phi^\circ$ [3b] is replaced by the delay $\Delta = 1/(2J_{CH})$ between (b) and (c) in Fig. 2. The corresponding modification in the phase cycle of the receiver is also presented in Fig. 2. Although this pulse sequence could be performed by applying gradients in the same manner as published earlier,[3b] we present data in this study using the pulse sequence without any gradients as shown in Fig. 2. The reason for this is as follows: the $1/T_{1\rho}$ values are related with $1/T_2$, $1/T_{1\rho} \approx \cos^2\ \theta(1/T_2)$[3c,13a–c] with $\theta = \tan^{-1}\ \{\Delta\omega_i/\gamma B_1\}$, where $\Delta\omega_i$ is the offset of ^{2}H from carrier and γB_1 is the strength of the spin-lock field. In the present study, we wished to observe the polarization transfer through the ^{2}H nuclei at the 2′ and 5′ centers. To neglect the offset effect in this case, the condition $\gamma B_1 \gg \Delta\omega_i$ should be fulfilled; $\Delta\omega_i$ is about 250 Hz. The spin-lock strength of about 1 kHz, as used in the earlier study[3] for CH_2D methyls of protein, was not sufficient in the present study to obtain monoexponential decay of $^{13}C_zD_y$ magnetization. To fulfil this condition, 11.4 or 2.6 kHz ^{2}H spin-lock field was tested using a triple TXO probe from Bruker with selective ^{13}C and ^{2}H channels with 40 and 11.4 kHz field strength of 90° pulses, respectively (see Experimental section).

Figure 3 shows [(A) and (C), obtained using pulse sequence (A) shown in Fig. 2] the ^{1}H–^{13}C correlation plot in H-2′/H-2″ and H-5′/H5″ regions of the double-labeled oligo-DNA duplex d5′(^{1}C^{2}G^3**A**^{4}**T**^{5}**T**^{6}**A**^{7}**A**^{8}**T**^{9}C^{10}G)$_2$3′ (**3**)] and its comparison with that of the natural counterpart (i.e. with natural abundance ^{13}C and proton) [(B) and (D)]. The experiment in Fig. 3(A) and (B) successfully allows us to select only those ^{13}C nuclei which have both proton and deuterium covalently attached [i.e. only diastereomeric C-2′ and C-5′ CHD carbons in ^{3}A, ^{4}T, ^{5}T, ^{6}A, ^{7}A and ^{8}T residues in oligo-DNA (**3**)], excluding the fully protonated 2′ and 5′ methylene carbons of non-deuterated residues (i.e. ^{1}C, ^{2}G, ^{9}C, ^{10}G).

In Fig. 2, the measurement of the relaxation rate of

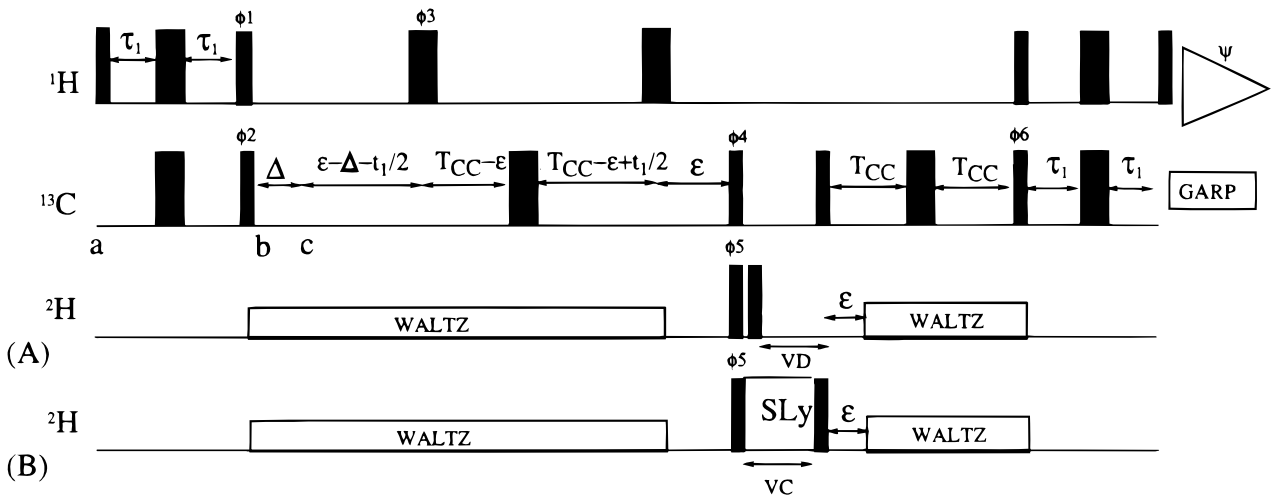

Figure 2. The pulse sequences employed for the measurements of T_1 and $T_{1\rho}$ relaxations of ^{2}H using TXO probe are shown in (A) and (B), respectively. In all sequences, narrow and wide pulses indicate 90° and 180° pulses, respectively, and unless indicated otherwise, all pulses are applied along the *x*-axis. The value of τ_1 was set to 1.79 ms [*ca* $1/(4J_{CH})$ with $J_{CH} = 140$ Hz], Δ was set to 3.57 ms [*ca* $1/(2J_{CH})$], ε was set to 11.4 ms [*ca* $1/(4J_{C^2H})$ with $J_{C^2H} = 22$ Hz] in all experiments. The constant time delay T_{CC} is inserted to eliminate ^{13}C–^{13}C splitting in the F_1 dimension, and it was set to 13.2 ms [*ca* $1/(2J_{CC})$ with $J_{CC} = 38$ Hz]. WALTZ decoupling[12a] of ^{2}H during pulsing was achived using a 1.3 kHz field. GARP[12b] decoupling of ^{13}C during acquisition was achieved using a 4.17 kHz field strength. The spin-lock strength of ^{2}H was 11.4 or 2.6 kHz. The phase cycling used for (A) ^{2}H (T_1), or for (B) ^{2}H ($T_{1\rho}$) experiments is $\phi_1 = y$; $\phi_2 = 8(x)$, $8(-x)$; $\phi_3 = 2(x)$, $2(-x)$; $\phi_4 = y$; $\phi_5 = 4(x)$, $4(-x)$; $\phi_6 = y$ and the receiver is $\psi = 4(x)$, $8(-x)$, $4(x)$. Quadrature detection in the F_1 dimension was achieved by States-TPPI on ϕ_3. Weak presaturation of the solvent was used in both sequences.

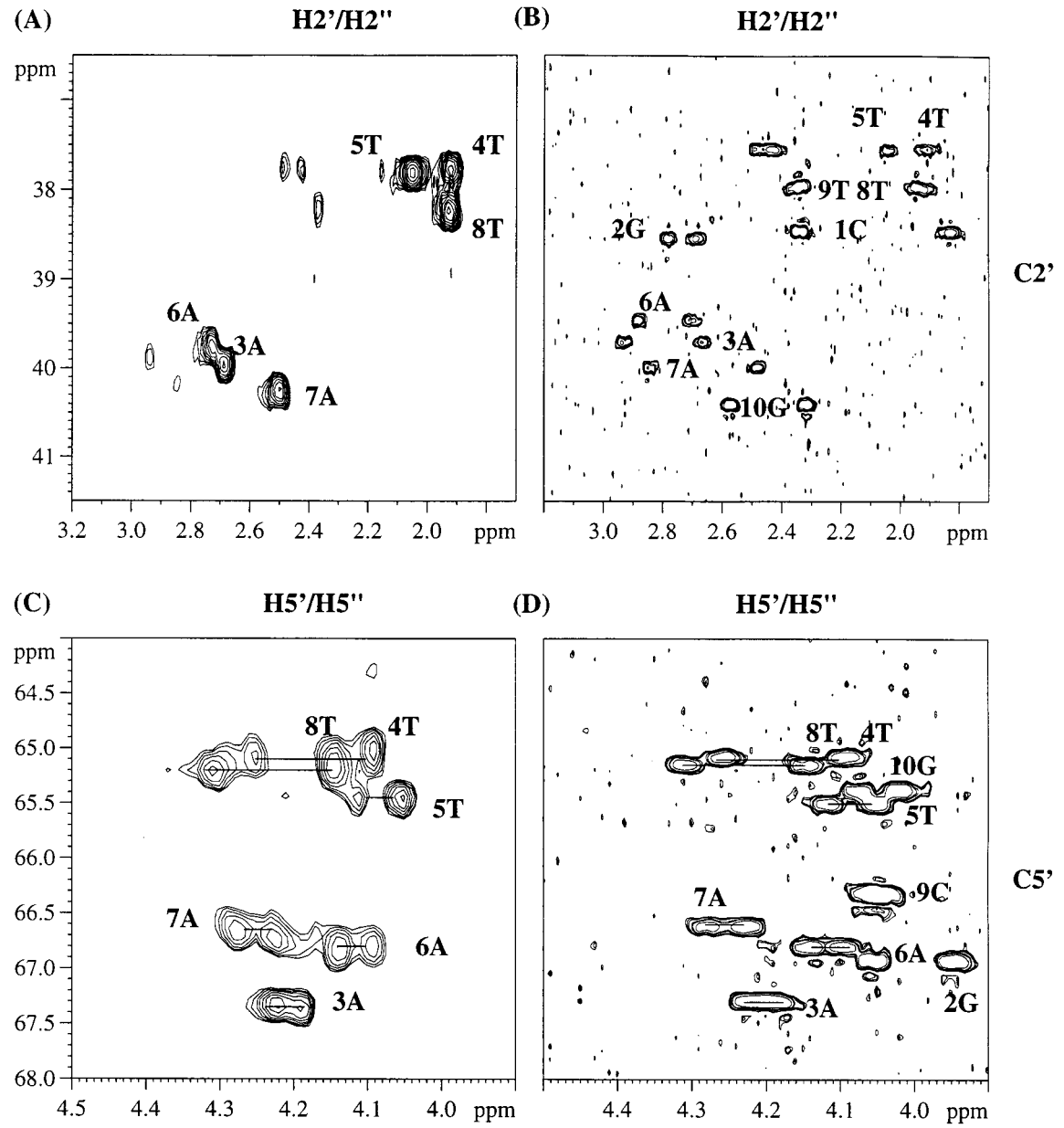

Figure 3. Comparison of the [^{1}H, (^{2}H), ^{13}C] correlation spectra of ^{2}H, ^{13}C double-labeled oligo-DNA duplex $d^{5'}(^1C^2G^3\underline{A}^4\underline{T}^5\underline{T}^6\underline{A}^7\underline{A}^8\underline{T}^9C^{10}G)_2^{3'}$[(A) and (C)], using the pulse sequence in Fig. 2(A), with that of standard [^{1}H, ^{13}C]-HSQC spectra of the counterpart in natural abundance [(B) and (D)]. The total measurement time of the [^{1}H, (^{2}H), ^{13}C] correlation experiment in (A) and (C) was *ca* 11 h: 256 × 2 K complex t_1 and t_2 points were acquired with acquisition times of 12.73 and 204.8 ms, respectively, with 64 scans. The experiment was employed with VD = 20 μs. For standard [^{1}H, ^{13}C]-HSQC, 2 K × 2 K complex t_1 and t_2 points were acquired with acquisition times of 113 and 204.8 ms, with 64 scans in *ca*. 46 h. The sweep width of the ^{13}C dimension was 80 ppm in the [^{1}H, (^{2}H), ^{13}C] experiment and 30 ppm in the [^{1}H, ^{13}C]-HSQC experiment; the carrier for ^{13}C was 55 and 75 ppm, respectively. (A) and (B) show the H-2′/H-2″–^{13}C region, whereas (C) and (D) show the H-5′/H-5″–^{13}C region.

$^{13}C_zD_z$ or $^{13}C_zD_y$ magnetization is presented but as has been shown,[3b,e] the relaxation times, T_1 and $T_{1\rho}$, of ^{2}H can be accurately calculated by subtraction of the relaxation rate of carbon from the $^{13}C_zD_z$/ or $^{13}C_zD_y$ relaxation rate:

$$1/T_1{}^D = 1/T_1^{(C_zD_z)} - 1/T_1^{(C_z)} \quad (3)$$

$$1/T_{1\rho}^D = 1/T_{1\rho}^{(C_zD_z)} - 1/T_1^{(C_z)} \quad (4)$$

In our experiments with 2′(*R*/*S*),5′(*R*/*S*)-$^2H_2$-1′,2′,3′,4′,5′-$^{13}C_5$-2′- deoxyadenosine (**1**) and the corresponding thymidine derivative (**2**), the T_1 relaxation of $^{13}C_z$ was about 900 ms, which corresponds to not more than 4% of overall $^{13}C_zD_z$/ or $^{13}C_zD_y$ relaxation.

T_1 and $T_{1\rho}$ of ^{2}H in 2′(*R*/*S*),5′(*R*/*S*)-$^2H_2$-1′,2′,3′,4′,5′-$^{13}C_5$-2′-deoxyadenosine (1) and the corresponding thymidine (2)

The errors in the data presented in Tables 1 and 2 represent the standard deviation of fitting the volume of

Table 1. Comparison of the longitudinal (T_1)[c] and transverse($T_{1\rho}$)[c] relaxation times (s) for ^{2}H in 1 and 2 at 11.7 T (TXO probe) at 298 K

Compound	Condition of experiments	Relaxation parameters	^{2}H(C-2′)[c]	^{2}H(C-5′)[c]	^{2}H(C-5″)[c]
1	5 mg in 0.6 ml D_2O	T_1	39.7 ± 0.6	36.1 ± 1.1	39.2 ± 1.3
		$T_{1\rho}$	39.7 ± 0.6	33.7 ± 0.8	37.4 ± 1.2
2	5 mg in 0.6 ml D_2O	T_1	57.2 ± 0.5	46.9 ± 1.2	48.9 ± 1.2
		$T_{1\rho}$	55.0 ± 0.9	39.4 ± 1.6	43.8 ± 2.5
2	30 mg in 0.6 ml D_2O	T_1	47.4 ± 0.8[a]	42.6 ± 1.6[a]	45.5 ± 1.5[a]
			44.8 ± 0.4[b]	42.4 ± 1.0[b]	41.3 ± 1.2[b]
		$T_{1\rho}$	43.9 ± 0.7	34.7 ± 2.0	35.4 ± 1.7

[a] First dataset obtained at a sweep width of ^{13}C of 80 ppm.
[b] Second dataset obtained at a sweep width of ^{13}C of 20 ppm.
[c] T_1 and $T_{1\rho}$ relaxation times were calculated from fitting the decay of magnetization C_zD_z and C_zD_y to the monoexponential curves; the presented error is the standard deviation of best fitting.

cross peaks to monoexponential decay. The random error was estimated using two independent datasets measured twice for T_1 of ^{2}H [Fig. 4(A), (C) and (E)] with the same sample (30 mg of **2** was chosen to ensure a high signal-to-noise ratio, and the error is not dictated by a poor signal-to-noise ratio) and TXO probehead (selective for ^{13}C and ^{2}H mode). In the first dataset, the sweep width was 80 ppm with carrier for ^{13}C at 55 ppm set equally for the ^{13}C(2′) and ^{13}C(5′) regions; in the second dataset, the carrier was set for ^{13}C(2′) at 40 ppm with a sweep width of 20 ppm [with folding of the ^{13}C(5′) area]. The relaxation times T_1 and $T_{1\rho}$ of ^{2}H obtained by fitting of the experimental data in Fig. 4 to an exponent are listed in Table 1. These data show that the random errors were less than 10%. Moreover, under the extreme narrowing limit[1] with $\omega\tau_{\text{eff}} \ll 1$ for isotropic motion with effective correlation time τ_{eff}, the relaxation times $T_1^Q \approx T_{1\rho}^Q$. Indeed, the experimentally measured T_1 and $T_{1\rho}$ deuterium relaxations for **1** are very close (less than 10% difference) for ^{2}H(2′). Noteworthy also is the observation that there is a minor difference between T_1 and $T_{1\rho}$ for ^{2}H(5′) or ^{2}H(5″).

Since both **1** and **2** have been incorporated into the oligo-DNA (**3**), we compared the relaxation times T_1 and $T_{1\rho}$ of ^{2}H for both nucleosides under identical conditions (5 mg of sample in 0.6 ml of D_2O). In Fig. 5, the experimental decays of ^{2}H(2′) [(A) and (B)], ^{2}H(5′) [(C) and (D)] and ^{2}H(5″) [(E) and (F)] of **1** (shown by circles) and **2** (shown by squares) are presented. From these data, it is clear that the relaxation time of deuterium for **1** is noticeably longer than that for **2**, which is especially true for ^{2}H(2′) (Table 1). In Table 2, the data for T_1 and

Table 2. Comparison of the longitudinal (T_1) and transverse ($T_{1\rho}$) relaxation times (s) for ^{2}H between different residues of decamer 3 at 11.7 T (TXO probe) at 298 K

Type of nucleus	Relaxation parameter	^{3}A	^{4}T	^{5}T	^{6}A	^{7}A	^{8}T
^{2}H(C-2′)	T_1	6.34 ± 0.20[a]	6.72 ± 0.35[a]	8.69 ± 0.35[a]	6.20 ± 0.45[a]	7.39 ± 0.37[a]	9.22 ± 0.44[a]
		6.24 ± 0.27[b]	6.73 ± 0.33[b]	8.56 ± 0.35[b]	5.95 ± 0.17[b]	6.38 ± 0.18[b]	9.13 ± 0.63[b]
		6.43 ± 0.77[c]	7.35 ± 0.22[c]	8.36 ± 0.38[c]	6.52 ± 0.78[c]	7.49 ± 0.38[c]	9.35 ± 0.37[c]
		(6.33 ± 0.26)[d]	(6.95 ± 0.19)[d]	(8.55 ± 0.20)[d]	(6.23 ± 0.28)[d]	(7.07 ± 0.20)[d]	(9.23 ± 0.26)[d]
	$T_{1\rho}$	1.69 ± 0.14[a]	1.62 ± 0.09[a]	2.10 ± 0.10[a]	1.41 ± 0.08[a]	1.36 ± 0.07[a]	1.83 ± 0.09[a]
		1.53 ± 0.14[b]	1.85 ± 0.11[b]	2.19 ± 0.09[b]	1.34 ± 0.04[b]	1.56 ± 0.03[b]	2.19 ± 0.14[b]
		1.45 ± 0.13[c]	1.83 ± 0.11[c]	1.97 ± 0.07[c]	1.67 ± 0.09[c]	1.59 ± 0.08[c]	1.94 ± 0.15[c]
		(1.57 ± 0.08)[d]	(1.76 ± 0.06)[d]	(2.11 ± 0.06)[d]	(1.47 ± 0.05)[d]	(1.50 ± 0.05)[d]	(1.90 ± 0.07)[d]
	T_1/T_ρ	4.03 ± 0.27	3.95 ± 0.20	4.05 ± 0.21	4.24 ± 0.28	4.71 ± 0.21	4.85 ± 0.27
^{2}H(C-5′)	T_1	7.11 ± 0.51	7.16 ± 0.57	7.21 ± 0.68	6.59 ± 0.50	7.76 ± 0.51	6.74 ± 0.64
	$T_{1\rho}$	1.44 ± 0.20	1.08 ± 0.07	1.03 ± 0.20	1.39 ± 0.30	1.73 ± 0.32	1.20 ± 0.11
^{2}H(C5″)	T_1	6.90 ± 0.47	6.34 ± 0.24	7.73 ± 0.72	7.45 ± 0.58	6.93 ± 0.51	7.21 ± 0.75
	$T_{1\rho}$	1.28 ± 0.18	1.36 ± 0.16	1.41 ± 0.15	1.47 ± 0.11	1.47 ± 0.22	1.31 ± 0.20

[a] The value with standard deviation obtained after fitting the experimental first dataset with a ^{13}C sweep width of 80 ppm. The carrier frequency in the ^{13}C dimension was set to 50 ppm (middle between 2′ and 5′ regions).
[b] The value with standard deviation obtained after fitting the experimental second dataset with a ^{13}C sweep width of 20 ppm. The carrier frequency in the ^{13}C dimension was set to 40 ppm (min. 2′ region).
[c] The value with standard deviation obtained after fitting the experimental third dataset with a ^{13}C sweep width of 20 ppm. The carrier frequency in the ^{13}C dimension was set to 40 ppm (min. 5′ region).
[d] The value with standard deviation obtained after fitting all the experimental datasets together.

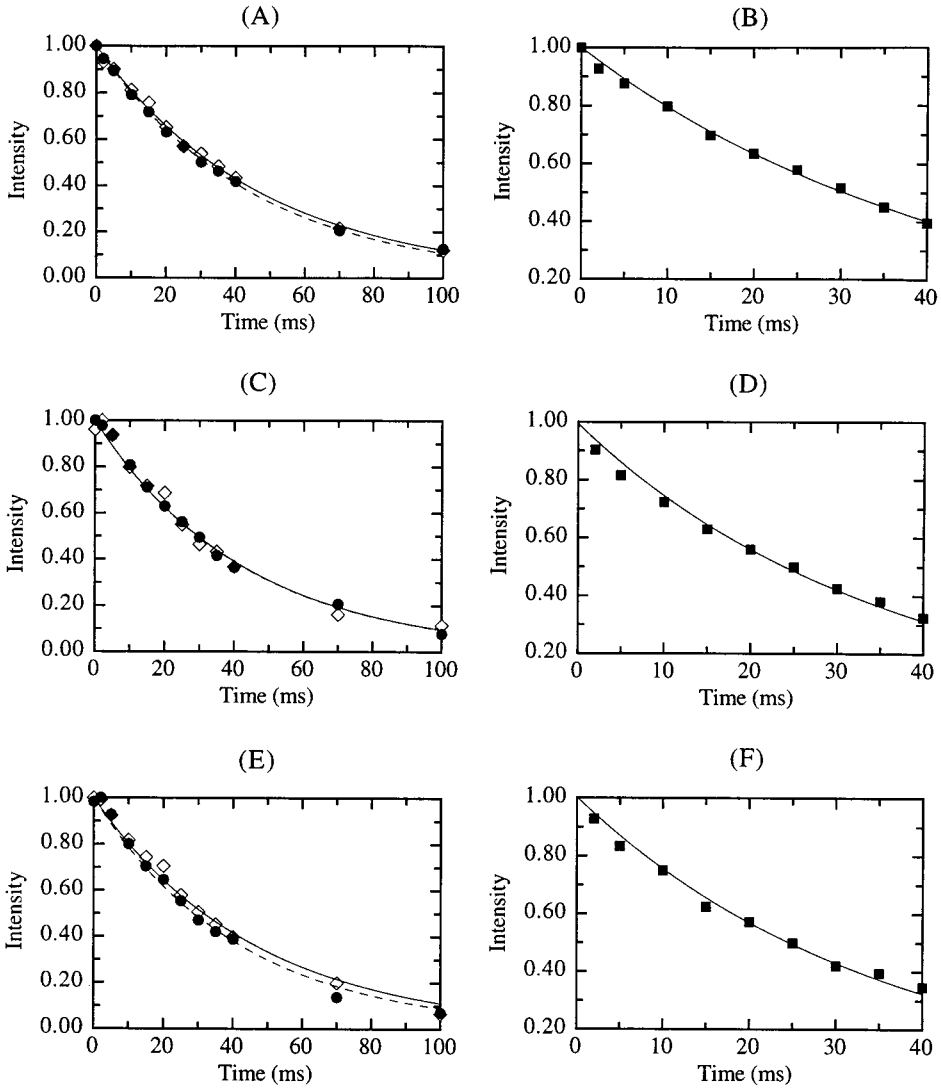

Figure 4. The normalized T_1 [(A), (C) and (E)] and $T_{1\rho}$ [(B), (D) and (F)] decay curves of ^{2}H for 2′(*R*/*S*),5′(*R*/*S*)-$^2H_2$-$^{13}C_5$-thymidine (**2**) (30 mg in 0.6 ml of D_2O) obtained from the volume of cross peaks in 2D spectra (NS = 16) as a function of the VD or VC delay in Fig. 2. (A) and (B) show the decay curves of the ^{2}H(2′) nucleus, (C) and (D) show the decay curves of the ^{2}H(5′) nucleus and (E) and (F) show the decay curves of the ^{2}H(5″) nucleus. The curves indicate best fits to single-exponential decays. Two experimental datasets with the same sample solution are shown by the symbols ● and ◇ in (A), (C) and (E): the first dataset was obtained with the carrier frequency in the ^{13}C(2′) region at *ca* 40 ppm and the second set was obtained in the ^{13}C(5′) region at *ca* 65 ppm. The spin-lock strength of ^{2}H was 2.6 kHz. The corresponding datasets, listed in Table 1, are best fitted and presented by solid and dashed lines.

$T_{1\rho}$ of ^{2}H in **1** and **2** are presented. Indeed, the ratio of T_1 or $T_{1\rho}$ of ^{2}H(2′) of T to that of 2′-dA residues is *ca* 1.4.

For selectively ^{13}C-1′ enriched protected nucleosides in DMSO-d_6, Paquet *et al.*[8d] report that their relaxation rates are similar. Obviously, the relaxation rates of *fully deprotected* nucleosides should be compared with native oligonucleotides in a very similar aqueous solution. It is likely that the bulky protecting groups used in cytosine, adenosine and guanine but *not* in thymidine affect the relaxation rates by changing both the bulk and the electronic characteristics that are specific for unprotected nucleosides. We, in this work, compared the deuterium relaxation of 2′-dA and T (i.e. completely unprotected) in aqueous solution as for oligonucleotide (under closely identical conditions) to show that their relaxation rates are indeed different. We performed an additional study (data not shown) of this phenomenon at different temperatures on various adenine, thimidine and cytosine nucleosides with different sites of deuterium incorporation both at the sugar and/or nucleobase. If the local mobility of the sugar versus nucleobase is indeed different in nucleoside level, then the energy of activation obtained from the relaxation rate measurement of deuterium as a function of inverse temperature is expected to be different. Indeed, the energies of activation for 2′-^2H-2′-deoxycytidine and 2′-^2H-thymidine residues were similar (21.6 kJ mol^{-1}), but it was 26.4 kJ mol^{-1} for 2′-^2H-2′-deoxyadenosine. This difference can be attributed to different mobility of sugar versus nucleobases around the glycosidic bond owing to the different bulk and electronic nature of the

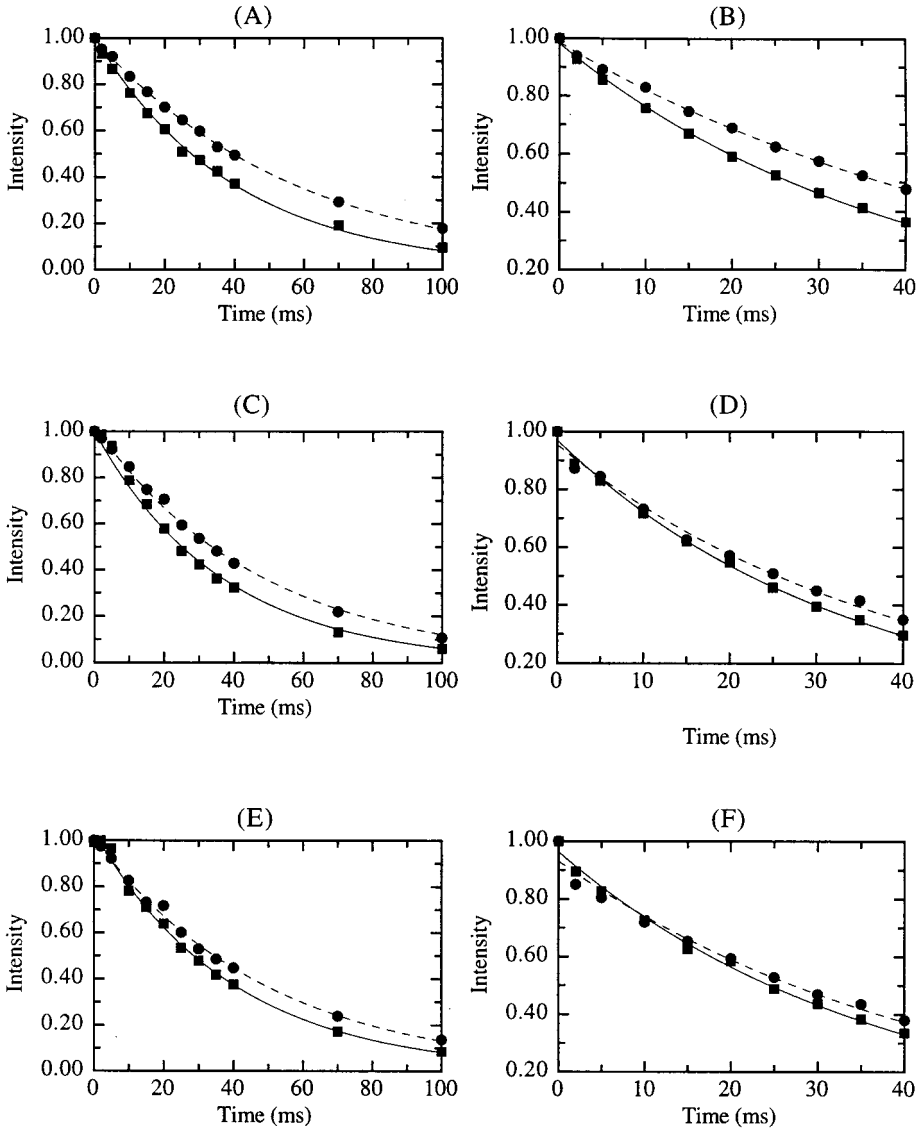

Figure 5. The normalized T_1 [(A), (C) and (E)] and $T_{1\rho}$ [Panels (B), (D) and (F)] decay curves of ^{2}H for 2′(*R*/*S*),5′(*R*/*S*)-$^2H_2$-$^{13}C_5$-2′-deoxyadenosine (**1**) (■) and 2′(*R*/*S*),5′(*R*/*S*)-$^2H_2$-$^{13}C_6$-thymidine (**2**) (●) (5 mg in 0.6 ml of D_2O) obtained from the volume of cross peaks in 2D (NS = 32) spectra as a function of the VD or VC delay in Fig. 2. The spin-lock strength of ^{2}H was 2.6 kHz. (A) and (B) show the decay curves of the ^{2}H(2′) nucleus, (C) and (D) show the decay curves of the ^{2}H(5′) nucleus and (E) and (F) show the decay curves of the ^{2}H(5″) nucleus. The data are presented in Table 1 and are best-fitted to single-exponential decays.

aglycone. The result of this study will be reported elsewhere in detail.

T_1 and $T_{1\rho}$ of ^{2}H in 2′(*R*/*S*),5′(*R*/*S*)-$^2H_2$-1′,2′,3′,4′,5′-$^{13}C_5$-2′-deoxyadenosine and the corresponding thymidine incorporated in the DNA decamer $d^{5'}(^1C^2G^3\underline{A}^4\underline{T}^5\underline{T}^6\underline{A}^7\underline{A}^8\underline{T}^9C^{10}G)_2^{3'}$

The experiment presented in Fig. 2 was applied to measure the relaxation times of ^{2}H nuclei of C-2′ and C-5′ methylene fragments in partially deuterated dA and T moieties in duplex **3**. The sensitivity of this experiment (Fig. 2) was illustrated by performing the measurement of the C_zD_z and C_zD_y magnetization of deuteromethylene fragments in dA and T residues with 1 mM double-labeled (^{2}H/^{13}C) DNA duplex in 0.6 ml of deuterium oxide. The three independent datasets collected (see Experimental condition and caption of Fig. 6) to measure the relaxation of the C_zD_z and C_zD_y magnetization by observing the decays of intensity of ^{1}H(2′)–^{13}C2′ cross peaks, depending upon the relaxation delay, are shown in Fig. 6. The extracted T_1 and $T_{1\rho}$ values of ^{2}H based on Eqns (3) and (4) at 298 K are presented in Table 2. The data show that the random error from the three experiments performed is $\leqslant$10%; the average values of T_1 or $T_{1\rho}$ of ^{2}H obtained using experimental data for all three datasets are presented in Table 2 with standard deviations of $\leqslant$3%. The same procedure was repeated to obtain T_1 and $T_{1\rho}$ values of ^{2}H at the 5′- and 5″-positions, and the final data are presented in Table 2. It is noteworthy that the standard

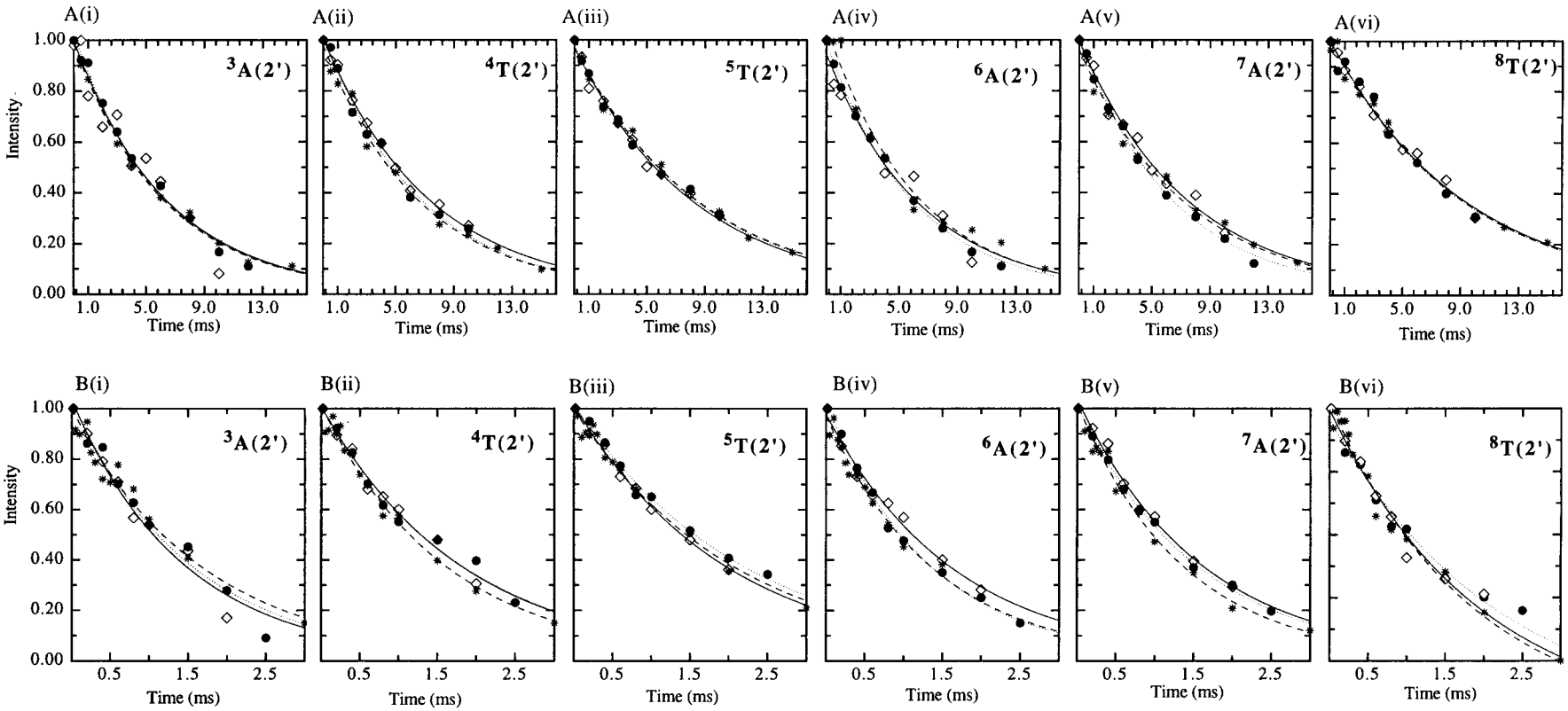

Figure 6. The normalized T_1 [A(i)–A(vi)] and $T_{1\rho}$ [B(i)–B(vi)] decay curves of ^{2}H(2′) for 2′(*R*/*S*),5′(*R*/*S*)-$^{2}H_2$-$^{13}C_5$-thymidine and the corresponding 2′-deoxyadenosine nucleotide residues (shown at the top right of each panel in bold) in the DNA duplex, $d^{5'}$ (^{1}C^{2}G^{3}**A**^{4}**T**^{5}**T**^{6}**A**^{7}**A**^{8}**T**^{9}C^{10}G)$_2^{3'}$ (1.3 mM in 0.6 ml of D_2O) at 298 K, obtained from the volume of cross-peaks in 2D spectra (at NS = 128 or 256 with a measurement time of *ca* 6 or 12 h for each spectrum, respectively) as a function of the VD or VC delay in Fig. 2. Three independent datasets are shown by the symbols ●, ◇ and ∗. The first dataset was obtained with the carrier frequency in the ^{13}C(5′,5″) region at *ca* 65 ppm, the second in the ^{13}C(2′) region at *ca* 40 ppm and the third between the ^{13}C(2′) and ^{13}C(5′) regions at *ca* 55 ppm. The spin-lock strength of ^{2}H ws 11.4 kHz. The corresponding best fits are presented by solid, dotted and dashed lines. The data are listed in Table 2.

deviation of T_1 and $T_{1\rho}$ of ^{2}H values in the 5′- and 5″-positions is larger than that for the 2′-position because the abundance of ^{2}H in the former (1:1 ratio) was approximately half of that of the latter (*ca* 85% ^{2}H).

The data presented in Table 2 allow two interesting observations. First, the ratios of T_1 of ^{2}H(2′) between T and dA nucleotides in A–T base pairs are 1.44 ± 0.12, 0.98 ± 0.09 and 1.37 ± 0.10 for ^{3}A–^{8}T, ^{4}T–^{7}A and ^{5}T–^{6}A, respectively.

It is likely that the slow, fast and overall motions in the nucleosides and in the oligonucleotides are different. Also, the relative contribution of these three different types of motions may be the origin of differences in various order parameters in the nucleosides and oligonucleotides. Hence the difference in the ratio between T and dA nucleosides and in the oligonucleotides could be tentatively attributed to two reasons: (1) the quadrupolar coupling constant of this nucleoside is different and (2) the order parameter between overall motion and local motion is different between nucleosides as well as in the oligonucleotides. It is noteworthy that the T_1 (res#1)/T_1 (res#2) ratios of both deuterium and ^{13}C relaxation of two nucleosides are different, suggesting that most probably the quadrupolar coupling constants are not the main reason for the said difference (note that in the solid state, the quadrupolar coupling constants, Q, decrease in the oligonucleotide level with increase in hydration; see Ref. 9). This suggests that most probably the difference in the order parameter of overall and local motions is the origin of difference in T_1 (res#1)/T_1 (res#2) ratios in various nucleosides and in oligonucleotides. It should be pointed out that one other probable reason for variable order parameters in nucleosides compared with oligonucleotides is that they have relatively different chemical environments as a result of stackings, H-bonding, hydration state and electrostatics in the latter (as has been postulated for the relaxation differences found between amino acids and proteins; see Ref. 14). The ratios for the first and third base pairs are very similar to those found in the free nucleosides (i.e. *ca* 1.4; see above).

The ratio in the second base-pair, however, is lower (note that the difference is larger than the experimental error!). The values for T_1 of ^{4}T and ^{7}A nucleoside are close to 7 ms. The T_1 for ^{4}T in **3** however, is lower by about 1.5 ms compared with other T nucleotide residues in the duplex. The T_1 for ^{7}A in **3**, however, is larger by 0.8 ms compared with other 2′-dA nucleotide residues in the duplex **3**. Clearly, the chemical environment inside an oligonucleotide is different than that which exists at a simple nucleoside level. It is noteworthy that a similar observation regarding differential mobilities for the adenine and thymine residues in oligo-DNA have been reported in a solid-state NMR study[9f] and ^{13}C relaxation studies.[8d–f]

Second, the $T_1/T_{1\rho}$ relaxation ratios are close to 4 for ^{3}A, ^{4}T and ^{5}T and slightly higher for ^{6}A and ^{7}A with value of 4.85 for ^{8}T. The difference in ^{13}C spin–spin relaxation rates $R(Cz_{x,y})$ among the residues in the 12 mer DNA with an AA tract has been observed earlier[8d–f] and explained by the slow motion of large variations of the nucleotide bending. In present study, at a spin-lock power of *ca* ~1316 Hz, the $T_{1\rho}$ decay curves of ^{2}H for all residues in our duplex as a function of delay represent a biexponential process, which could suggest an ongoing slow motion process for all nucleotide residues. Another possible explanation of this phenomenon is that the observed difference in the $T_1/T_{1\rho}$ ratio is due to the anisotropy of the duplex. The theoretical estimation has shown that the spectral density function change on orientation and axial ratio (i.e. number of base pairs) is significant even for a decamer DNA duplex.[10a]

Work is in progress to determine the T_1/T_2 of ^{13}C relaxation. Both deuterium and ^{13}C relaxations will then be used to determine the diffusion anisotropy of both 2′ and 5′ methylene fragments for each nucleotide residue within the duplex, which will in turn allow the determination of long-range order in NMR structure.

EXPERIMENTAL

Synthesis of double-labeled ^{13}C/^{2}H nucleosides

The non-stereoselective incorporation of deuterium at C-5′ was achieved via oxidation[15] of the 5′-OH group in 2′,3′-*O*-isopropylidene-N^6-benzoyladenosine-1′,2′,3′,4′,5′-$^{13}C_5$ and 1-(2′,3′-*O*-isopropylidene-β-D-ribofuranosyl-1′,2′,3′,4′,5′-$^{13}C_5$)thymine prepared from uniformly labeled D-glucose-$^{13}C_6$ (A. Földesi and J. Chattopadhyaya, to be published) followed by reduction of the resulting aldehyde with sodium borodeuteride. Deuterium labeling of C-2′ was carried out by reductive elimination of the phenoxythiocarbonyl group[16] to afford the double-labeled key building blocks N^6-benzoyl-2′-deoxyadenosine-2′(*R*/*S*),5′(*R*/*S*)-$^2H_2$-1′,2′,3′.4′,5′-$^{13}C_5$ and thymidine-2′(*R*/*S*),5′(*R*/*S*)-$^2H_2$-1′,2′,3′,4′,5′-$^{13}C_5$ after removal of the 1,1,3,3-tetraisopropyldisiloxan-1,3-diyl[17] protection. These 2′-deoxynucleoside blocks were converted into the appropriate phosphoramidite derivatives.[18] All intermediates were satisfactorily characterized by ^{1}H, ^{13}C and ^{31}PNMR spectra recorded on a Jeol JNM GX 270 spectrometer at 270.17, 67.94 and 109.37 MHz, respectively.

DNA synthesis and purification

The double-labeled 10-mer (**3**) was prepared by the solid-phase phosphoramidite method on a Pharmacia LKB Gene Assembler Special synthesizer. The standard 1.3 μmol scale programs were modified to have a 2 min coupling time. After deprotection in 32% aqueous ammonia solution for 2 days at 45 °C, the solvent was evaporated. The residue was dissolved in water and extracted (three times) with dichloromethane and finally with diethyl ether. Purification of the oligomer was carried out on a DEAE-Sephadex A-25 column with a linear gradient of 0–0.3, 0.3–0.6 and 0.6–1.0 M ammonium-hydrogencarbonate solution (500 ml each). After checking by reversed-phase HPLC (Gilson system consisting of Model 305 and 306 pumps, Model 811C dynamic mixer and Model 118 UV detector) on a Kromasil 100-5C_{18} (250 × 8 mm i.d.) reversed-phase column with a linear gradient of 0–40% buffer B [0.1 M triethylammonium acetate (TEAA) (pH 6.8), 50% CH_3CN] in buffer A [0.1 M TEAA (pH 6.8), 5% CH_3CN] over a period of 40 min, appropriate fractions were pooled and desalted by repeated co-evaporation with water. Finally, the purified sample (237 absorbance units, 13%) was loaded on a Dowex 50W-X (Na^+ form) column, then lyophilized together with the appropriate buffer used for NMR spectroscopy from D_2O (99.9% D).

NMR experiments

The NMR experiments were carried out on a Bruker DRX spectrometer (11.7 T) operating at 500.023 MHz

for ^{1}H, 125.73 MHz for ^{13}C and 76.76 MHz for ^{2}H. The spectrometer was equipped with a Bruker digital lock and triple-resonance selective probe for ^{13}C and ^{2}H (TXO). All ^{1}H pulses were applied with a 24 kHz field and all ^{13}C pulses with a 40 kHz field. This strength of ^{13}C pulses allowed us to excite the region between ^{13}C(5′) and ^{13}C(2′) resonances and neglect the offset effect on measurement of T_1 and T_2 relaxation of ^{13}C, as we showed earlier in a relaxation study on deuterated nucleosides.[19] ^{13}C decoupling was performed using GARP with a 4.17 kHz field strength.

The spectrometer was equipped with a switching ^{2}H lock–^{2}H pulse device. The probe power after the switching block was 43.0 W for the 90° and 180° ^{2}H pulses, which corresponds to an 11.4 kHz applied field. ^{2}H decoupling utilized a WALTZ16 sequence using a 1.3 kHz field (0.6 W) and a 11.4 or 2.6 kHz ^{2}H spin-lock field (SL_y) (Fig. 2) was used in the $T_{1\rho}$ measurements.

Carriers were positioned at 4.8 ppm for ^{1}H and ^{2}H in all experiments; 65 ppm in the area of ^{13}C(5′) and 40 ppm in area of ^{13}C(2′) or 55 ppm for ^{13}C depending on the experiment. The spectra were recorded with acquisition times of 15.5 and 204.8 ms in (t_1, t_2) in 78 × 2048 or 12.7 and 204.8 ms in (t_1, t_2) 256 × 2048 complex matrices depending upon the sweep width used for carbon, 20 or 80 ppm, respectively.

A relaxation delay of 2 s was employed. The relays used in pulse sequences are given in the caption of Fig. 2.

To avoid spinning artefacts, all spectra were measured on non-spinning samples.

Data evaluation in 2D experiments

The spectra were processed and analyzed on a Silicon Graphics workstation using XWINNMR version 2.1 and AURELIA programs of Bruker software. Apodization, zero-filling and Fourier transformation led to a digital resolution of 1.23 Hz per point in the F_1 and 2.44 Hz per point in the F_2 dimension for experiments with SW (^{13}C) = 20 ppm and 4.91 Hz per point in the F_1 and 2.44 Hz per point in the F_2 dimension for experiments with SW(^{13}C) = 80 ppm. For the evaluation of the T_1 or $T_{1\rho}$ relaxation time, the volume of cross peaks in the series of 2D spectra [^{1}H(^{2}H)^{13}C] were fitted to a single exponential, depending on the relaxation delay, using the equation

$$V(\Delta) = V(0)\exp(-\Delta/T_i) \quad (5)$$

where T_i is the relaxation rate T_1 or $T_{1\rho}$ and $V(\Delta)$ and $V(0)$ are the volume of cross peaks at time Δ (defined in Fig. 2 as VD or VC) and zero time, respectively.

$T_1(C_zD_z)$ values were based on measurements from 14 spectra recorded with VD delays between 20 μs and 15 ms for the oligo-DNA duplex $d^{5'}(^1C^2G^3\underline{A}^4\underline{T}^5\underline{T}^6\underline{A}^7\underline{A}^8\underline{T}^9C^{10}G)_2^{3'}$ (**3**) and between 20 μs and 100 ms for nucleosides (**1** and **2**). $T_{1\rho}(C_zD_y)$ values were measured from the average of 11 or 14 spectra recorded with VC delays between 20 μs and 2.5 ms for the oligo-DNA duplex $d^{5'}(^1C^2G^3\underline{A}^4\underline{T}^5\underline{T}^6\underline{A}^7\underline{A}^8\underline{T}^9C^{10}G)_2^{3'}$ (**3**) and between 20 μs and 40 ms for nucleosides (**1** and **2**).

The fit was performed using a least-squares minimization procedure using the program PROFIT 4.2. The monoexponential character of decay was tested using Monte Carlo procedures according to the literature.[20]

Acknowledgements

Authors thank the Swedish Board for Technical and Engineering Research (TFR), the Swedish Natural Science Research Council (NFR contract #K-KU 12067-300 to AF&K-AA/Ku04626-321 to JC) and the Wallenbergsstiftelsen for generous financial support.

REFERENCES

1. A. Abraham, *Principles of Nuclear Magnetism.* Clarendon Press, Oxford (1961).
2. See, for example: (a) L. K. Lee, M. Rance, W. J. Chazin and A. G. Palmer, III, *J Biomol. NMR* **9**, 287 (1997); (*b*) G. Wagner, *Nature Struct. Biol.* **2**, 255 (1995); (c) A. G. Palmer, III, *Curr. Opin. Biotechnol.* **4**, 385 (1993); (d) K. T. Dayie, G. Wagner and J. K. Lefevre, *Annu. Rev. Phys. Chem.* **447**, 243 (1996); (e) L. K. Nicolson, T. Yamazaki, D. A. Torchia, S. Grzesiek, A. Bax, S. J. Stahl, J. D. Kaufman, P. T. Wingfield, P. Y. Lam, P. K. Jadhav, C. N. Hodge, P. J. Domaille and C. H. Chang, *Nature Struct. Biol.* **2**, 274 (1995); (f) A. M. Mandel, M. Akke and A. G. Palmer, III, *J. Mol. Biol.* **246**, 144 (1995); (g) D. T. Browne, G. L. Kenyon, E. L. Packer, H. Sternlicht and D. M. Wilson, *J. Am. Chem. Soc.* **95**, 1316 (1973); (h) J. Engelke and H. Ruterjans, *J. Biomol. NMR* **9**, 63 (1997).
3. D. Yang, L. E. Kay, *J. Magn. Reson.* SB **110**, 213 (1996); (b) D. R. Muhandiram, T. Yamazaki, B. D. Sykes and L. E. Kay, *J. Am. Chem. Soc.* **117**, 11536 (1995); (c) T. Yamazaki, W. Lee, C. H. Arrowsmith, R. Muhandiram and L. E. Kay, *J. Am. Chem. Soc.* **116**, 11655 (1994); (d) T. Yamazaki, R. Muhandiram and L. E. Kay, *J. Am. Chem. Soc.* **116**, 8266, (1994); (e) D. R. Muhandiram, P. E. Johnson, D. Yang, O. Zhang, L. P. McIntosh and L. E. Kay, *J. Biomol. NMR* **10**, 283, (1997); (*f*) D. Yang, A. Mittermaier, Y.-K. Mok and L. E. Kay, *J. Mol. Biol.* **276**, 939 (1998).
4. (a) S. Grzesiek, A. Anglister, H. Ren and A. Bax, *J. Am. Chem. Soc.* **115**, 4369 (1993); (b) S. Grzesiek, P. Wingfield, S. Stahl, J. D. Kaufman and A. Bax, *J. Am. Chem. Soc.* **117**, 9594 (1995); (c) A. C. Wang, S. Grzesiek, R. Tschudin, P. J. Lodi, A. Bax, *J. Biomol. NMR* **5**, 376 (1995).
5. (a) J. P. Malthouse and M. D. Finucane, *Biochem. J.* **280**, 649 (1991); (b) K. Pervushin, G. Wider and K. Wuthrich, *J. Am. Chem. Soc.* **119**, 3842 (1997).
6. (a) A. Földesi, F. P. R. Nilson, C. Glemarec, C. Gioeli and J. Chattopadhyaya, *Tetrahedron* **48**, 9033 (1992); (b) A. Földesi, F. P. R. Nilson. C. Glemarec, C. Gioeli and J. Chattopadhyaya, *J. Biochem. Biophys. Methods* **26**, 1 (1993); (c) S.-i. Yamakage, T. V. Maltseva, F. P. R. Nilson, A. Földesi and J. Chattopadhyaya, *Nucleic Acids Res.* **21**, 5005 (1993); (d) P. Agback, T. V. Maltseva, S.-i. Yamakage, F. P. R. Nilson, A. Földesi and J. Chattopadhyaya, *Nucleic Acids Res.* **22**, 1404 (1994); (e) A. Földesi, S.-i. Yamakage, T. V. Maltseva, F. P. Nilson, P. Agback and J. Chattopadhyaya *Tetrahedron* **51**, 10065 (1995); (f) A. Földesi, S.-I. Yamakage, F. P. R. Nilsson, T. V. Maltseva and J. Chattopadhyaya, *Nucleic Acids Res.*, **24**, 1187 (1996); (g) C. Glemarec, J. Kufel, A. Földesi, T. Maltseva, A. Sandström, L. A. Kirsebom and J. Chattopadhyaya, *Nucleic Acids Res.*, **24**, 2022 (1996); (h) E. Kawashima, K. Toyama, K. Ohshima, M. Kainosho, Y. Kyogoku and Y. Ishido, *Tetrahedron Lett.* **36**, 6699 (1995); (i) Y. Oogo, M. A. Ono, S.-i. Tate, A. S. Ono and M. Kainosho, *Nucleic Acids Symp. Ser. 37*, 35, (1997); (j) A. Ono, T. Makita, S.-I. Tate, E. Kawashima, Y. Ishido, M. Kainosho, *Magn. Reson. Chem.* **34**, S40 (1996); (k) S.-i Tate, Y. Kubo, A. Ono, M. Kainosho, *J. Am. Chem. Soc.* **117**, 7277 (1995); (l) C. Kojima, E. Kawashima, K. Toyama, K. Ohshima, Y. Ishido, M. Kainosho and Y. Kyogoku, *J. Biomol. NMR* **11**, 103, (1998); (m) E. Kawashima, Y. Aoyama, T. Sekine, M. Miyahara, M. F. Radwan, E. Nakamura, M. Kainosho,

Y. Kyogoku and Y. Ishido, *J. Org. Chem.*, **60**, 6980 (1995); (n) A. Ono, A. Ono and M. Kainosho., *Tetrahedron Lett.* **38**, 395 (1997); (o) A. Ono, (M.); T. Shiina, A. Ono and M. Kainosho, *Tetrahedron Lett.* **39**, 2793 (1998); (p) X. Huang, P. Yu, E. LeProust and X. Gao, *Nucleic Acids Res.* **25**, 4758 (1997); (q) T. J. Tolbert and J. R. Williamson, *J. Am. Chem. Soc.* **118**, 7929 (1996); (p) J. J. De Voss, J. J. Hangeland and C. A. Townsend, *J. Org. Chem.* **59**, 2715 (1994); (r) E. P. Nikonowicz, M. Michnicka and E. DeJong, *J. Am. Chem. Soc.* **120**, 3813 (1998); (s) J. M. Louis, R. G. Martin, G. M. Clore and A. M. Gronenborn, *J. Chem. Biol.* **273**, 2374 (1998); (t) T. J. Tolbert and J. R. Williamson, *J. Am. Chem. Soc.* **119**, 12100 (1997); (u) S. Quant, R. W. Wechselberger, M. A. Wolter, K.-H. Wörner, P. Schell, J. W. Engels, C. Griesinger and H. Schwalbe, *Tetrahedron Lett.* **35**, 6649 (1994); (v) L. A. Agrofoglio, J-C. Jacquinet, G. Lancelot, *Tetrahedron Lett.* **38**, 1411 (1997); (z) A. S. Serianni and P. B. Bondo, *Biomol. Struct. Dy.* **11**, 1133 (1994).

7. (a) R. T. Batey, J. L. Battiste and J. R. Williamson, *Methods Enzymol.* **261**, 300 (1995); (b) A. Pardi, *Methods Enzymol.* **261**, 350 (1995); (c) G. C. King, J. W. Harper and Z. Xi, *Methods Enzymol.* **261**, 436 (1995); (d) K. B. Hall, *Methods Enzymol.* **261**, 542 (1995); (e) K. T. Dayie, T. J. Tolbert and J. R. Williamson, *J. Magn. Reson.* **130**, 97 (1998).
8. (a) G. Mer and W. J. Chazin, *J. Am. Chem. Soc.* **120**, 607 (1998); (b) J. M. Louis, R. G. Martin, G. M. Clore, A. M. Gronenborn., *J. Biolog Chem.* **273**, 2374 (1998); (c) D. P. Zimmer, J. P. Marino, C. Griesinger, *Magn. Reson. Chem.* **34**, S177 (1996); (d) F. Paquet, F. Gaudin and G. Lancelot, *J. Biomol. NMR* **8**, 252 (1996); (e) F. Gaudin, L. Chanteloup, N. T. Thuong and G. Lancelot, *Magn. Reson. Chem.* **35**, 561 (1997); (f) F. Gaudin, F. Paquet, L. Chanteloup, J.-M. Beau, N. T. Thuong and G. Lancelot, *J. Biomol. NMR* **5**, 49 (1995).
9. (a) B. H. Robinson and G. P. Drobny, *Methods Enzymol.* **261**, 451 (1995); (b) T. M. Alam, J. Orban and G. P. Drobny, *Biochemistry* **30**, 9229 (1991); (c) W.-C. Huang, J. Orban, A. Kintanar, B. R. Reid and G. P. Drobny, *J. Am. Chem. Soc.* **112**, 9059 (1990); (d) R. Brandes, R. R. Vold, D. R. Kearns and A. Rupprecht, *A. Biochemistry* **29**, 1717 (1990); (e) S. Roy, Y. Hiyama, D. Torchia and J. S. Cohen, *J. Am. Chem. Soc.* **108**, 1675 (1986); (f) D. G. Brown, M. S. Sanderson, E. Garman and S. Neidle, *J. Mol. Biol.* **226**, 481 (1992).
10. (a) A. N. Lane, *Methods Enzymol.* **261**, 413 (1995); (b) N. Tjandra, D. S. Garrett, A. M. Gronenborn, A. Bax and G. M. Clore, *Nature Struct. Biol.* **4**, 443 (1997); (c) M. W. F. Fisher, L. Zeng, Y. Pang, W. Hu, A. Majumdar and E. R. P. Zuiderweg *J. Am. Chem. Soc.* **119**, 12629 (1997); (d) H. H. Mantsch, H. Saito and I. C. P. Smith, *Prog. Nucl. Magn. Reson. Spectrosc.* **11**, 211 (1977); (e) G. M. Clore, A. M. Gronenborn, A. Szabo and N. Tjandra, *J. Am. Chem. Soc.* **120**, 4889 (1998).
11. (a) D. S. Goodsell, M. Kaczor-Grzeskowiak and R. E. Dickerson, *J. Mol. Biol.* **239**, 79 (1994); (b) J. R. Quintant, K. Grzeskowiak, K. Yanagi and R. E. Dickerson, *J. Mol. Biol.* **225**, 379 (1992).
12. (a) A. J. Shaka, J. Keeler, T. Frenkiel and R. Freeman, *J. Magn. Reson.* **52**, 335 (1983); (b) A. J. Shaka, P. B. Barker and R. Freeman, *J. Magn. Reson.* **64**, 547 (1985).
13. (a) J. W. Peng, V. Thanabal and G. Wagner, *J. Magn. Reson.* **95**, 421 (1991); (b) J. W. Peng, V. Thanabal and G. Wagner, *J. Magn. Reson.* **98**, 308 (1992); (c) T. E. Bull, *Prog. Nucl. Magn. Reson. Spectrosc.* **24**, 377 (1992).
14. J. Boyd, T. K. Mal, N. Soffe and I. D. Campbell, *J. Magn. Reson.* **124**, 61 (1987).
15. R. S. Ranganathan, G. H. Jones and J. G. Moffatt, *J. Org. Chem.* **39**, 290 (1974).
16. (a) M. J. Robins, J. S. Wilson and F. Hansske, *J. Am. Chem. Soc.* **105**, 4059 (1983); (b) A. Földesi, F. P. R. Nilson, C. Glemarec, C. Gioeli and J. Chattopadhyaya, *Tetrahedron* **48**, 9033 (1992).
17. W. T. Markiewicz, *J. Chem. Res.* (*S*) 24 (1979).
18. (a) A. D. Barone, J.-Y. Tang and M. H. Caruthers, *Nucleic Acids Res.* **12**, 4051 (1984); (b) W. Bannwarth and A. Trzeciak, *Helv. Chim. Acta* **70**, 175 (1987); (c) N. D. Sinha, J. Biernat, J. McManus and H. Köster, *Nucleic Acids Res.* **12**, 4539 (1984).
19. T. V. Maltseva, A. Földesi and J. Chattopadhyaya, *J. Magn. Reson. Chem.* **36**, 227 (1998).
20. (a) A. G. Palmer, III, M. Rance and P. E. Wright, *J. Am. Chem. Soc.* **113**, 4371 (1991); (b) L. K. Nicholson, L. E. Kay, D. M. Baldisseri, J. Arango, P. Young, A. Bax, D. A. Torchia, *Biochemistry* **31**, 5253 (1992).